# Improved In-line VIV Prediction for Combined In-line and Cross-flow VIV Responses

**Decao Yin***
SINTEF Ocean
Trondheim, NO-7052
Norway
Email: decao.yin@sintef.no

**Elizabeth Passano**
SINTEF Ocean
Trondheim, NO-7052
Norway

**Carl M. Larsen**
SINTEF Ocean/NTNU
Trondheim, NO-7052
Norway

## ABSTRACT

Slender marine structures are subjected to ocean currents, which can cause vortex-induced vibrations (VIV). Accumulated damage due to VIV can shorten the fatigue life of marine structures, so it needs to be considered in the design and operation phase.

Semi-empirical VIV prediction tools are based on hydrodynamic coefficients. The hydrodynamic coefficients can either be calculated from experiments on flexible beams by using inverse analysis or theoretical methods, or obtained from forced motion experiments on a circular cylinder. Most of the forced motion experiments apply harmonic motions in either in-line (IL) or cross-flow (CF) direction. Combined IL and CF forced motion experiments are also reported. However, measured motions from flexible pipe VIV tests contain higher order harmonic components, which have not yet been extensively studied.

This paper presents results from conventional forced motion VIV experiments, but using measured motions taken from a flexible pipe undergoing VIV. The IL excitation coefficients were used by semi-empirical VIV prediction software VIVANA to perform combined IL and CF VIV calculation. The key IL results are compared with Norwegian Deepwater Programme (NDP) flexible pipe model test results. By using present IL excitation coefficients, the prediction of IL responses for combined IL and CF VIV responses is improved.

Nomenclature
$A_{CF}$ Amplitude in cross-flow direction.
$A_{IL}$ Amplitude in in-line direction.
$A_y$ Amplitude in y (cross-flow) direction.
$A/D$ Non-dimensional amplitude.
$C_D$ Drag coefficient.
$C_{D0}$ Drag coefficient of a fixed cylinder.
$D$ Diameter.
$\bar{F}_{IL}$ Mean force in the IL direction.
$f_n$ Natural frequency.
$f_{osc}$ Oscillation frequency.
$f_v$ Vortex shedding frequency.
$\hat{f}$ Non-dimensional oscillation frequency.

*Corresponding author.

$L$ Length.
$R$ Radius.
$Re$ Reynolds number.
$U$ Current or towing velocity.
$v_{IL/CF}$ Displacement in in-line or cross-flow direction.
$Y_{RMS}$ Root-mean-square of displacement in y direction.
$\sigma_{IL,disp,max}$ Spatial maximum standard deviation of in-line displacement.
$\sigma_{IL,mean}$ Spatial mean IL stress.
$\varepsilon$ Strain.
$\kappa$ Curvature.
$\varphi$ Phase angle between in-line and cross-flow motions.
$\omega$ Angular frequency.
$\omega_i$ The $i^{th}$ angular frequency.
$\omega_{osc}$ Angular oscillation frequency.
2D Two dimensional.
CF Cross-flow.
CFD Computational fluid dynamics.
DNS Direct numerical simulation.
DOF Degree of freedom.
IL In-line.
NDP Norwegian Deepwater Programme.
VIV Vortex-induced vibrations.
VIVANA A vortex-induced vibrations prediction program.

## 1 Introduction

When flow pasts cylindrical offshore structures, vortices are generated and shedding into the wake, cyclic vortex force will cause vibrations of the structures, such vibrations are called vortex-induced vibrations (VIV). Research activities on VIV have been carried out by several research groups for decades. Most of the state-of-the-art VIV prediction tools are semi-empirical, SHEAR7 [1], VIVA [2] and VIVANA [3] are all VIV prediction programs in frequency domain, and they are based on hydrodynamic coefficients obtained from experiments. Pure CF forced VIV experiments were done by [4] on a rigid circular cylinder at $Re = 10^4$. These excitation coefficients have been widely used to predict pure CF VIV responses and, in some cases, also used to predict the CF part of combined IL and CF VIV responses. Pure IL VIV forced VIV experiments were carried out at $Re = 2.4 \times 10^4$ [5]. Pure IL excitation coefficients obtained from these experiments have been used to predict pure IL VIV responses, but are not valid for prediction of the IL part of combined IL and CF responses. Forced motion tests with two dimensional (2D) harmonic motions have been carried out by [6]. Different frequency ratios were achieved by tuning frequency in CF and IL independently. It was found that the phase angle between CF and IL is an important factor, with regard to higher order forces.

Realistic orbits measured from a flexible beam VIV model tests were applied in forced motion VIV model tests [7]. This experimental method was first applied by [8], and further used by [7] and [9]. Both non-periodic time history of the motions and representative periodic motions were used in the experiments, see Fig. 2. The hydrodynamic coefficients from the periodic motion tests were calculated and presented in [10]. The sensitivity of the hydrodynamic force and vortex shedding modes on the different realistic orbits were investigated in [11]. It was found that harmonic orbits had larger uncertainties to predict VIV than realistic orbits, and that IL motions can result in large higher order force components. Results from non-periodic and periodic forced motion VIV tests were compared in [12]. Depending on the response types, for quasi-periodic VIV responses, periodic orbits are representative for non-periodic time histories; while when the responses are partly or fully chaotic, the hydrodynamic coefficients calculated from tests with selected periodic orbits have larger uncertainty or fail to represent the entire time history.

VIV tests on flexible beams have been carried out [13] [14] [15]. In these tests, accelerometers and strain gauges are usually instrumented on the flexible beams, so that acceleration and bending strain are measured. But, the hydrodynamic forces could not be measured directly. Since displacement is known, hydrodynamic forces can be obtained by applying inverse analysis [16]. Hydrodynamic force calculated by inverse analysis can be used to enrich and improve the hydrodynamic coefficient database based on forced motion experiments. In [15], hydrodynamic forces were theoretically calculated by Euler-Bernoulli beam vibration equation, and the hydrodynamic coefficient were further investigated.

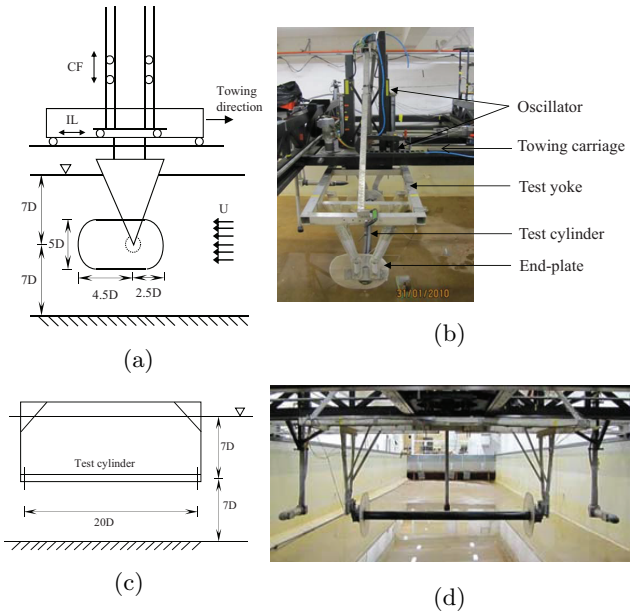


Fig. 1: Sketch and photos of test set-up of forced motion VIV tests in NTNU MC-Lab.

Computational fluid dynamics (CFD) is a useful tool to understand the wake of flow and fluid-structure interaction. Three dimensional direct numerical simulation (DNS) was performed on a flexible beam subjected to linearly and exponentially sheared currents at relative low Reynolds number [17]. Multi-frequency responses were observed in both cases, but with different spectral contents. There are a lot of other CFD studies using various turbulent models instead of DNS. Challenges of CFD are high quality mesh, long calculation time and validation versus experiments. Hence, there are still some limitations to use CFD method to analyse a real slender structure such as a riser or a pipeline.

In this paper, 2D forced motion VIV tests were performed on a rigid cylinder. Realistic orbits were used in the experiments. IL excitation coefficients were extracted and applied by a semi-empirical VIV prediction tool VIVANA, to predict the IL VIV responses of a flexible beam under both uniform and sheared currents.

## 2 Experimental Method

### 2.1 Set-up

The forced motion experiments were carried out in the NTNU Marine Cybernetics Laboratory (MC-Lab) [18]. The MC-lab is a small tank with dimensions ($L \times B \times D$) of 40 $m \times 6.45$ $m \times 1.5$ $m$. The tank is equipped with an overhead towing carriage. Six degrees-of-freedom (DOF) forced motions can be achieved by a computer controlled system. In present tests, only IL and CF motions were applied to the tested model.

The test set-up of forced motion VIV tests is shown in Fig. 1. This apparatus was first designed and applied by [5]. A test yoke was attached to the towing carriage. Target IL and CF oscillatory motions were achieved by moving the yoke horizontally and vertically while the carriage was towed. For each test, the motions of the towing carriage and the test model were input by an input file to the host computer which remotely controlled the motions.

The test model is a rigid steel cylinder with an outer diameter of 10 cm and a length of 2 m, giving a length-to-diameter ratio of 20. The detailed properties of the cylinder model are shown in Tab. 1. The cylinder was mounted to the yoke. The two ends of the cylinder were capped to keep the cylinder air filled and the cylinder mass as low as possible. Two end plates ($7D \times 5D$) were installed to reduce three-dimensional end effects. The two end plates were in-line with the towing direction and parallel to each other, to ensure a 2D uniform current.

Two force sensors were mounted orthogonally at both ends to measure the forces in the IL and CF directions. The IL and CF displacements of the cylinder were measured by two potentiometers.

It is vital to have a rigid test rig (high stiffness) so that measured signals are not influenced. Pluck tests were carried out both in air and in water. The natural frequency of the test rig is higher than 6 Hz in water, and higher than 30 Hz in air [7]. The natural frequency of the test rig is significantly larger than the oscillation frequency of the forced motion VIV tests (smaller than 1 Hz), therefore, bandpass filtering was applied when post-processing the signals.

Table 1: Properties of the test model in forced motion VIV tests.

| Property | Dimension |
|---|---|
| Length, $L$ | 2 m |
| Outer diameter, $D$ | 2 m |
| Mass in air | 9.775 kg |
| Outer surface | Painted |

2.2 Scaling

Reynolds number scaling was used between the NDP high mode VIV tests and the present forced motion VIV experiments. The Reynolds number is defined as:

$$Re = \frac{UD}{\nu} \tag{1}$$

where $U$ is the current/towing velocity, $\nu$ is the kinematic viscosity.

The non-dimensional oscillation frequency is defined as:

$$\hat{f} = \frac{f_{osc}D}{U} \tag{2}$$

where $f_{osc}$ is the oscillation frequency.

In addition, the non-dimensional amplitude $A/D$ in both IL and CF directions and non-dimensional oscillation frequency were kept the same.

2.3 Orbits

Forced motion VIV experiments have been carried out extensively in the past several decades. In most of these experiments harmonic motions were applied in CF and/or in IL directions. These harmonic motion can be expressed by:

$$v_{CF}(t) = A_{CF}sin(\omega t) \tag{3}$$

$$v_{IL}(t) = A_{IL}sin(\omega t + \varphi) \tag{4}$$

where $v_{CF}$ and $v_{IL}$ are displacements in CF and IL directions respectively, $A_{CF}$ and $A_{IL}$ are motion amplitudes in CF and IL directions respectively, $\omega_{osc} = 2\pi f_{osc}$ is angular oscillation frequency, $\varphi$ is the phase angle between IL and CF motions.

However, measured motions from flexible beam VIV tests are rarely harmonic, due to the stochastic nature of VIV response. Higher order frequency components are often observed in the measured displacements of points on a flexible beam undergoing VIV. The CF and IL displacement time series can be expressed by Fourier series including a number of frequency components:

$$v_{IL/CF}(t) = \frac{a_{IL/CF,0}}{2} + \sum_{i=1}^{\infty}[a_{IL/CF,i}cos(\omega_i t) + b_{IL/CF,i}sin(\omega_i t)] \tag{5}$$

At each frequency $\omega_i = 2i\pi/T$, the CF and IL motions can be expressed in a similar way as Eq. 3 Eq. 4, more detail description of Eq. 5 can be found in [7].

Table 2: Physical properties of pipe model in NDP high mode VIV tests.

| Property | Dimension |
|---|---|
| Total length between pinned ends | 38.00 m |
| Outer diameter | 27 mm |
| Wall thickness of pipe | 3.0 mm |
| Bending stiffness, EI | 37.2 $Nm^2$ |
| Young modulus for pipe, E | $3.62 \times 10^{10}$ $Nm^2$ |
| Axial stiffness, EA | $5.09 \times 10^5$ $N$ |
| Mass (air filled), measured | 0.761 $kg/m$ |
| Mass (water filled), estimated | 0.933 $kg/m$ |
| Mass ratio | 1.62 |
| Pre-tension | 4000-6000 N |

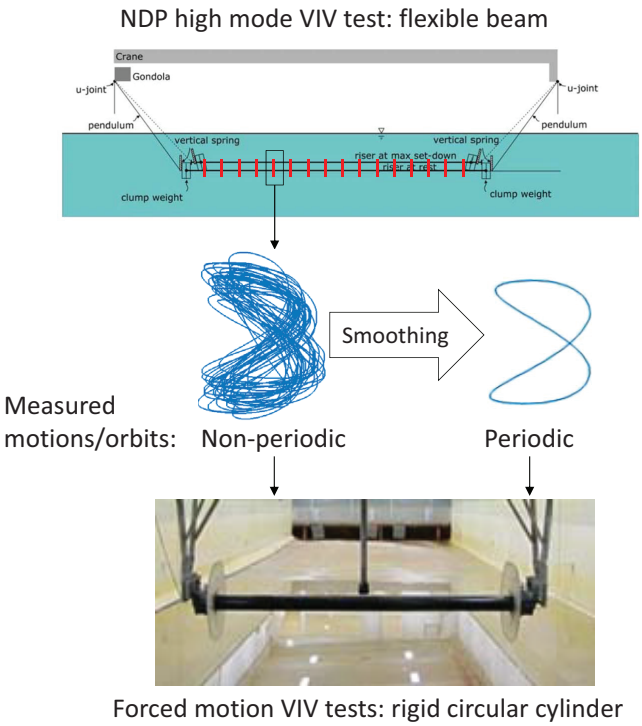


Fig. 2: Illustration of application of measured non-periodic and periodic orbits in forced motion VIV tests.

In these forced motion VIV experiments, the forced motions were based on measured motions of selected cross sections of the flexible beam of the NDP high mode VIV model tests [13]. In the NDP high mode VIV tests, a 38 m long flexible beam was towed in the Ocean Basin in MARINTEK. Uniform and sheared flows were generated by towing both or one end of the beam. Bending strains and accelerations along the model were recorded and applied to calculate displacements and curvature [13]. The key properties of NDP model tests are presented in Tab. 2.

The measured motions within selected time windows can be applied directly in forced motion VIV experiments, and this type of orbits are denoted 'non-periodic observed orbits'. Periodic orbits are desired for identification of force coefficients, measured motions of two successive periods were smoothed to be closed (periodic) orbits, and this type of orbits are denoted 'periodic observed orbits' [10] [11] [12]. This process is illustrated in Fig. 2.

2.4 Data acquisition and sampling

The effective length of the MC-Lab towing tank is 20 m. Each rigid cylinder forced motion test lasted between 50 s and 4 min, depending on the towing velocity. All measured signals were sampled at a frequency of 400 Hz. The beginning and the end of the time series were always removed when calculating hydrodynamic coefficients to eliminate transient effects.

2.5 Data analysis

Drag coefficient

The drag coefficient is defined by the mean force in the IL direction:

$$C_D = \frac{\bar{F}_{IL}}{\frac{1}{2}\rho DLU^2} \tag{6}$$

where $\bar{F}_{IL}$ is the mean force in the IL direction, $\rho$ is the density of the fluid.

Excitation coefficient

The dynamic excitation coefficient of each harmonic component $\omega_n$ is defined as:

$$C_{e,IL/CF,n} = \frac{\lim_{k\to\infty} \frac{\int_t^{t+kT} F_{h,IL/CF,n}(\tau)\cdot \dot{v}_{IL/CF,n}(\tau) d\tau}{kT}}{\frac{1}{4}\rho DLU^2 \omega_n v_{IL/CF,n,0}} \tag{7}$$

where $v_{IL/CF,n}(\tau)$ and $F_{h,IL/CF,n}(\tau)$ are the filtered displacement and filtered hydrodynamic force time series at $\omega_n$ respectively. Both of them have a frequency bandwidth around the nth order frequency component $\omega_n$. $v_{IL/CF,n,0}$ is the amplitude of motion at frequency component $\omega_n$, $T$ is the oscillation period, integer number of oscillation periods $kT$ are used to calculate the excitation and added mass coefficients.

This force coefficient defines the energy transfer between fluid and cylinder for each harmonic component present in the time series. A positive coefficient value means that energy is transferred from the fluid to the cylinder, while a negative coefficient indicates energy dissipation through hydrodynamic damping.

Added mass coefficient

The added mass coefficients define the harmonic component of the hydrodynamic force in phase with the respective acceleration components, and are defined as:

$$C_{a,IL/CF,n} = -\frac{\lim_{k\to\infty} \frac{\int_t^{t+kT} F_{h,IL/CF,n}(\tau)\cdot \ddot{v}_{IL/CF,n}(\tau) d\tau}{kT}}{\frac{1}{8}\rho D^2 L \omega_n^4 v_{IL/CF,n,0}^2} \tag{8}$$

3 Data analysis of NDP high mode VIV tests

Modal analysis/model decomposition was performed thoroughly on all NDP high mode VIV tests in [13], and the results from are further used for comparison in this paper. Both bending strain and acceleration signals were used in the modal analysis. Detail description of the model analysis method can be found in [13].

From modal analysis, the modal weight standard deviations were calculated with respect to either displacement or curvature, and dominating mode was identified by finding out the largest value of modal weight standard deviation with respect to curvature.

Displacement and curvature have been reconstructed using the calculated modal weights. The curvature is further processed to stresses by using the relationship $\kappa = \varepsilon/R$, where $\kappa$ is curvature, $\varepsilon$ is strain, and $R$ is the radius of the flexible beam.

4 IL Prediction for Combined IL & CF VIV

IL VIV response is significantly larger in combined IL & CF VIV than in pure IL VIV, and it leads to considerable fatigue damage, which can be as much as the fatigue damage due to CF response, or even higher. Pure IL excitation coefficients are not valid to predict IL in combination with CF response.

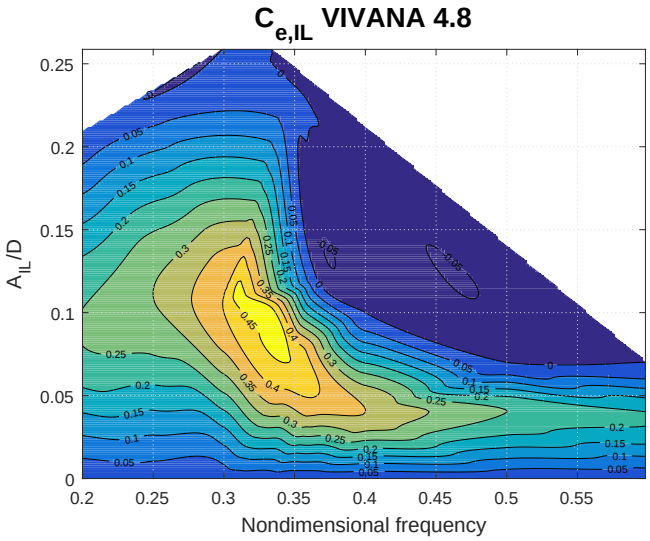


Fig. 3: Default IL coefficients for a combination of CF and IL responses in VIVANA 4.8.

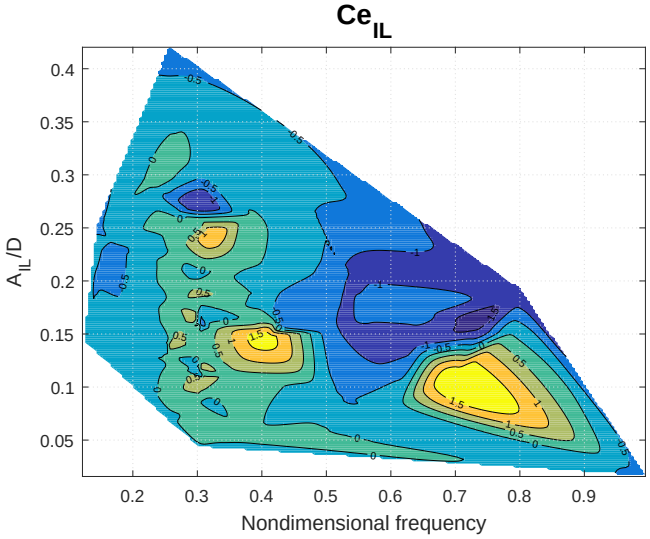


Fig. 4: IL coefficients obtained from forced motion VIV experiments using realistic orbits from NDP high mode VIV model tests.

### 4.1 Excitation coefficients

The default IL excitation coefficients in VIVANA 4.8 for combined IL and CF responses are presented as a contour plot in Fig. 3. This database is based on the results from the PhD work of Soni [8], and is updated based on comparisons with the model tests on a vertically tensioned riser [19] [20]. The coefficients should still be considered as preliminary. It is seen that the excitation region has non-dimensional frequency range from 0.25 to 0.6, the maximum excitation coefficient is around 0.5, the maximum amplitude ratio with zero excitation coefficient is 0.22.

Figure 4 shows the IL coefficients obtained from forced motion VIV experiments using realistic periodic orbits from the NDP high mode VIV model tests.

Unlike the default IL excitation coefficient database, there are two excitation regions in the excitation coefficients from the present study. In the 1st instability region, $\hat{f}$ ranges from 0.62 to 0.91 and has a maximum $A_{IL}/D$ of approximately 0.15 at approximately $\hat{f} = 0.75$. The 2nd instability region ranges from 0.2 to 0.5 and has a maximum $A_{IL}/D$ of approximately 0.15 at approximately $\hat{f} = 0.4$. These two regions are equivalent to those found by [5], which are results from pure IL VIV experiments.

This study also found a third instability region around the amplitude ratio of 0.25. These amplitudes are not present for the pure IL response, but they are often found for the combined IL and CF cases.

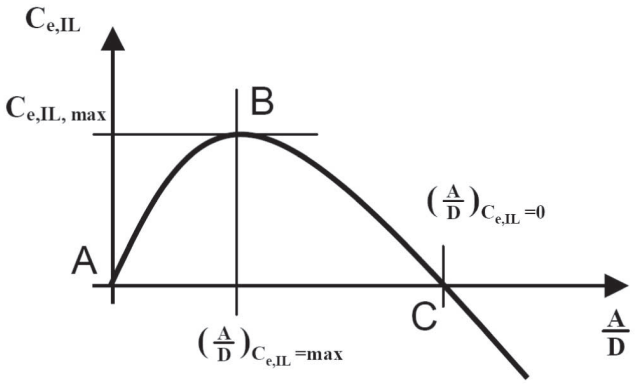


Fig. 5: The IL excitation coefficient curve at single non-dimensional frequency in VIVANA [3].

The results are hence realistic and useful to identify the excitation coefficients for the IL response in combination with the CF response.

In addition, the second instability region is much wider, and there is a large gap between the two regions. Both regions have a much larger amplitude ratio in the IL direction. This high $A_{IL}/D$ also appears in the IL excitation coefficient contour plot of [3]. The differences between the contour plots from pure IL experiments and the current study indicate that the CF component has a strong influence on the forces in the IL direction.

However, the coefficients shown in Fig. 4 can not be directly used in VIVANA. The built-in excitation coefficient in VIVANA is defined as a function of amplitude ratio for a given non-dimensional frequency, see the solid black curve in Fig. 5. This curve is composed of two second order polynomial AB and BC, which are defined by three points A, B and C [3]:

1. Point A gives the excitation coefficient value when response amplitude ratio equals to zero, $C_{e,IL,A/D=0}$.
2. Point B is defined by the maximum excitation coefficient, $C_{e,IL,max}$, and corresponding amplitude ratio $(A/D)|_{C_{e,IL,max}}$. Note that both polynomials have zero gradients at this point.
3. Point C defines the $A/D$ value when excitation coefficient equal to zero, $(A/D)|_{C_{e,IL}=0}$. This amplitude ratio corresponds to the amplitude ratios along the zero contour lines in Fig. 3.

The excitation coefficients in Fig. 4 were simplified and smoothed. During this process, a sub-area in Fig. 4 is selected to capture the excitation region. This area has the non-dimensional frequency range from 0.24 to 0.9, and $A_{IL}/D$ ranges from 0 to 0.26. At every non-dimensional frequency, the excitation coefficients should be represented by three points A, B and C shown in Fig. 5. An effort is done to define the three points at discrete non-dimensional frequencies, this is the smoothing process. The modified coefficients used in this paper are presented as contour plot in Fig. 6.

## 5 Results and Discussions

In this paper, combined IL and CF VIV analysis were performed by using the semi-empirical VIV prediction software VIVANA 4.8 [3]. The consecutive frequency (time sharing) response option is chosen.

Key VIV prediction results are generated from VIVANA using both the default and the updated IL coefficients, and compared to the experimental results. The other parameters and settings are kept identical, in order to see the performance of the updated IL coefficients. For the same reason, the VIV responses in CF will not be discussed in this paper.

Comparisons are made on selected cases of the NDP high mode VIV tests. The selected tests for comparison are listed in Tab. 3, seven(7) sheared flow cases and seven (7) uniform flow cases. Among them, the six tests whose orbits were used in the forced motion VIV experiments are marked.

### 5.1 Dominating mode

The dominating IL response modes are shown in Fig. 7 (shear flow) and Fig. 8 (uniform flow). Note that the number of data points is the same for each series, but 'VIVANA 4.8' and 'VIVANA Updated' predict the same mode number for some cases, where the data points of 'VIVANA Updated' are on top of 'VIVANA 4.8' data points, so that it looks like there are fewer data points for the latter. For the experiments, the mode is estimated from the shape of the displacement standard deviation. For the VIVANA analyses, the mode number corresponding

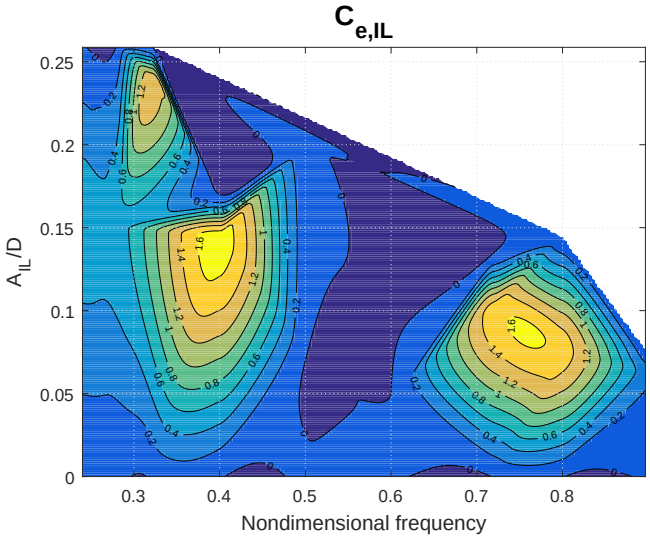


Fig. 6: Modified IL coefficients obtained from forced motion VIV experiments using realistic orbits from NDP high mode VIV model tests.

Table 3: Selected tests from the NDP High Mode VIV tests for comparison.

| Test No. | U (m/s) | Orbits | Flow |
|---|---|---|---|
| 2330 | 0.5 | | |
| 2340 | 0.6 | x | |
| 2360 | 0.8 | | |
| 2370 | 0.9 | x | Shear |
| 2400 | 1.2 | | |
| 2430 | 1.5 | x | |
| 2450 | 1.7 | | |
| 2020 | 0.4 | | |
| 2030 | 0.5 | x | |
| 2060 | 0.8 | | |
| 2100 | 1.2 | x | Uniform |
| 2130 | 1.5 | | |
| 2160 | 1.8 | x | |
| 2182 | 2.0 | | |

to the response frequency with the largest responses reported. For both shear and uniform flow case, VIVANA slightly over-predict the dominating mode. This over-prediction is larger for uniform flow cases than the sheared flow cases, especially when the towing speed is high.

When performing combined IL and CF VIV analysis, VIVANA first find the dominating CF response frequency by iteration until the response frequency is consistent with the updated CF added mass coefficient. The response frequency with the highest ranking factor is assumed to be the dominating response frequency and assigned the largest relative duration.

The IL added mass is then adjusted in order to obtain a dominating IL response frequency which is exactly twice the dominating CF response frequency. The same IL response frequency will be found regardless of whether the default or the updated IL excitation coefficients are used, since the CF excitation and added mass coefficients

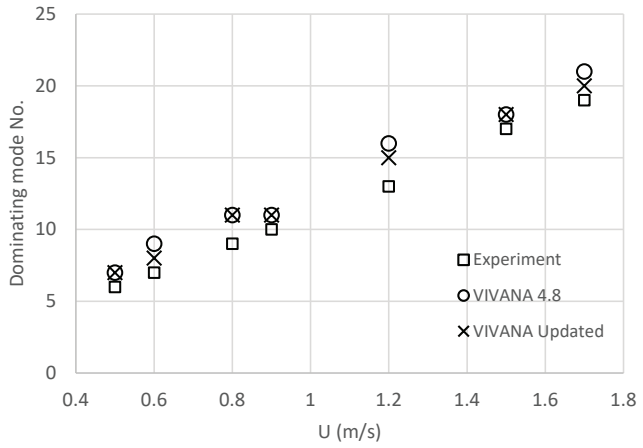


Fig. 7: Dominating IL mode comparison, shear flow cases.

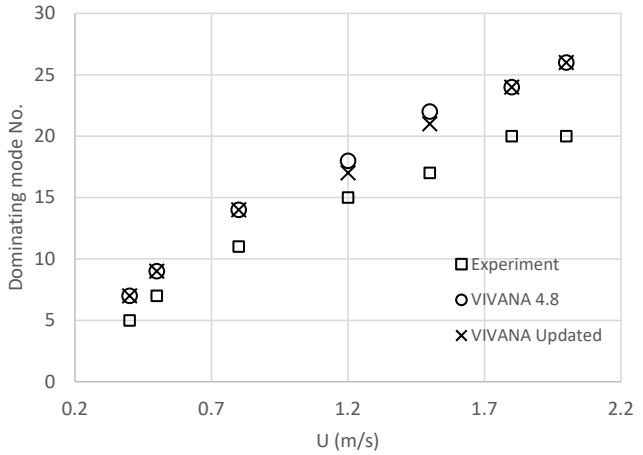


Fig. 8: Dominating IL mode comparison, uniform flow cases.

are identical. The slight difference of one mode number for five of the fourteen cases is due to that the target double frequency falls in between two initial natural frequencies and that VIVANA select one instead of the other.

5.2 IL displacement

The responses of the flexible pipe in the NDP high mode VIV tests were reconstructed using the strain and acceleration measurements [13]. Standard deviation of the IL displacement was calculated along the pipe, and the maximum value of the IL displacement standard deviation is compared with the VIVANA calculation.

The comparison for the shear flow cases is shown in Fig. 9, and the comparison for the uniform flow cases is shown in Fig. 10. Generally, VIVANA underestimates the standard deviation of IL displacements for both shear and uniform flow cases. For shear flow cases, VIVANA using the updated excitation coefficients improve the prediction and gives less non-conservative predictions.

There is a difference between the shear flow cases and the uniform flow cases. Assume that the response frequency is the same along the pipe. For shear flow cases, the non-dimensional frequency varies along the pipe and the excitation region is easy to determine. However, for uniform flow cases, the entire pipe has the same non-dimensional frequency, which makes it more challenging to determine the excitation region and damping region. For example, non-symmetric responses are observed for uniform flow cases, while it is not obvious to predict which side the excitation region will be on.

It is seen from Fig. 10 that the predicted results from VIVANA using the updated coefficients exhibit more scattering. To investigate it, the non-dimensional frequencies of all uniform flow cases are plotted in the contour plot of the updated IL coefficients, see Fig. 11. All the uniform flow cases are seen to have non-dimensional frequencies range from 0.23 to 0.34, in the region where two excitation regions with different amplitude ranges were found from the experiments with measured orbits. The modified (smoothed) excitation curves used in the

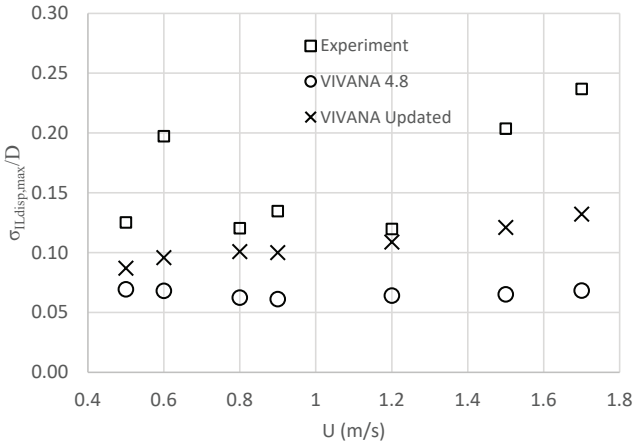


Fig. 9: Maximum standard deviation of IL displacement along the pipe, normalized by the outer diameter, shear flow cases.

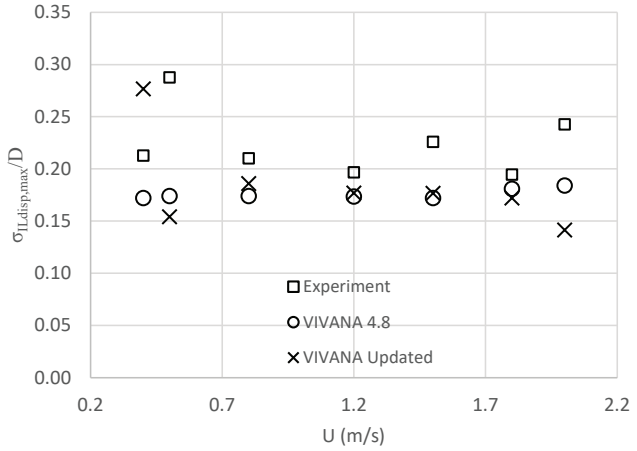


Fig. 10: Maximum standard deviation of IL displacement along the pipe, normalized by the outer diameter, uniform flow cases.

VIVANA analyses are therefore more uncertain in this region.

### 5.3 IL stress

The micro-strain of the flexible pipe in the NDP high mode VIV tests were measured in both IL and CF directions. Standard deviation of the IL stress was calculated along the pipe [13], and the mean value of the standard deviation IL stress is compared with the VIVANA calculation. The reason to compare the mean values instead of maximum values is due to that only the mean values from experimental measurements are available. As the stresses from the experiments include higher order components that VIVANA does not attempt to include, some discrepancy between experimental and predicted stress must be expected.

The comparison of shear flow cases is shown in Fig. 12, and the comparison of uniform flow cases is shown in Fig. 13.

For the shear flow cases in Fig. 12, the default IL excitation coefficients give non-conservative stress compared to the experimental results. Using the updated coefficients, the predicted IL stress increases to about twice the default, and matches the experimental measurements for the cases with towing speed from 0.5 m/s to 1.2 m/s.

For the uniform flow cases in Fig. 13, both default and updated coefficients give conservative IL stress, compared to the experimental measurements. The difference between the prediction using the two sets of coefficients is small. The predicted mean standard deviations of stress with updated coefficients are slightly higher than with the default coefficients, which indicates results are more conservative.

In general, by using updated IL coefficients in combined IL and CF VIV predictions, the predicted IL responses are improved significantly compare to the default coefficients.

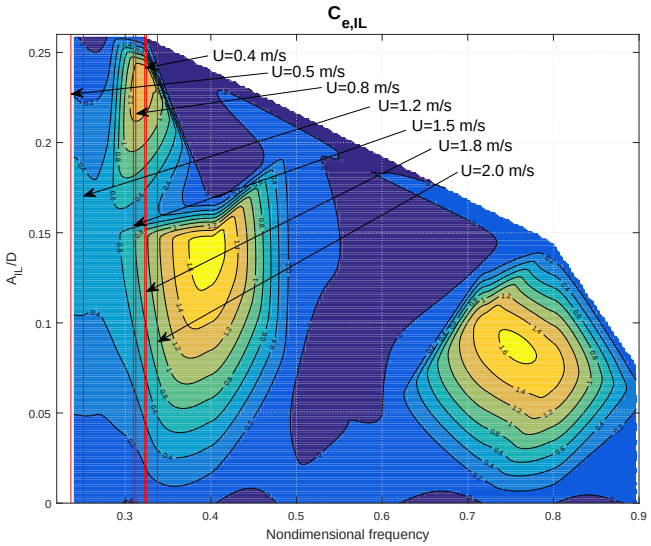


Fig. 11: Non-dimensional frequencies of uniform flow cases in the modified IL excitation coefficient contour plot.

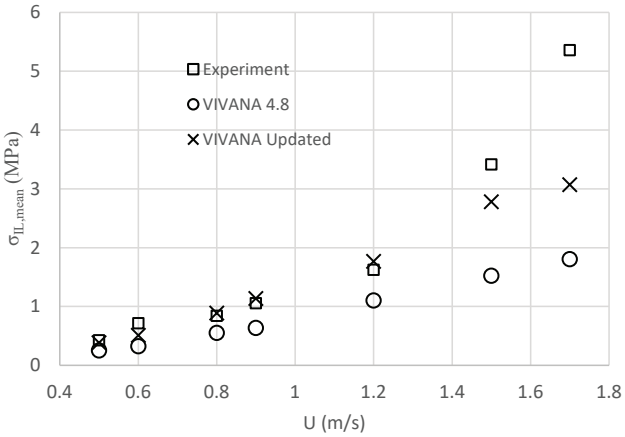


Fig. 12: Spatial average of standard deviation of IL stress, shear flow cases.

it is important to note that, the reconstructed displacement and curvature contain not only the dominating mode, but also several other participating modes. In the present VIVANA calculation, 'time sharing' option was selected, which means that response frequencies act consecutively. More detail modal analysis may improve the comparison, this will be taken into account in the further study.

## 6 Conclusions

A series of forced motion experiments were conducted in MC-Lab of NTNU, Trondheim. Different from conventional harmonic motions, periodic and non-periodic measured motions from the NDP high mode VIV tests were used in the experiment. Hydrodynamic coefficients were extracted and the IL excitation coefficients are used in this study. The phase angle between IL and CF motions and higher motion components are not explicitly included in the coefficient database, but are implicitly included when the forced motion experiments were carried out. A semi-empirical VIV prediction tool is used in this study to carry out combined IL and CF VIV analysis. Both the default IL excitation coefficients and the updated IL coefficients were used, and predicted results were compared to experimental measurements.

Comparison is made for selected NDP high mode VIV tests, including both the cases from which the orbits applied in the forced motion tests were taken from, and other cases The comparison shows that by using the updated IL coefficients, the IL responses of combined IL and CF VIV response are predicted better, with regard to the conservation of the standard deviation of displacement and stress. This study suggests the updated coefficients are applicable in combined IL and CF VIV prediction and shows that the forced motion experiments using measured

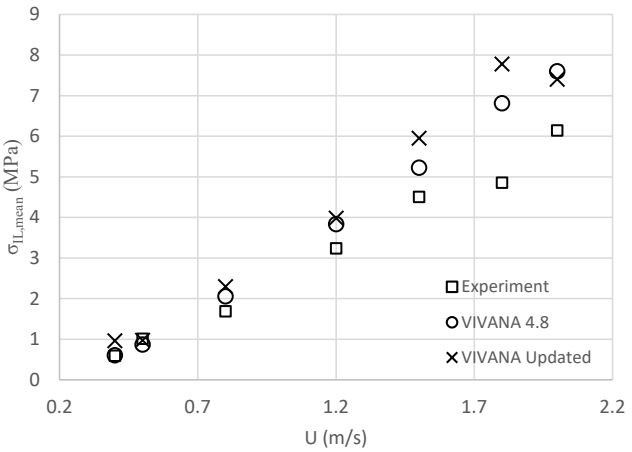


Fig. 13: Spatial average of standard deviation of IL stress, uniform flow cases.

orbits are effective methods for obtaining excitation coefficients.

It is important to note that the updated IL excitation coefficient database is still based on limited number of forced motion VIV experiments. A more comprehensive hydrodynamic coefficient database is needed to improve the VIV prediction, especially the IL coefficients for combined IL and CF VIV. The hydrodynamic coefficient database should be tested, calibrated and optimized against other flexible model tests before used in industry.

Acknowledgements

The authors wish to express their gratitude to NDP for permission to publish the results from NDP high mode VIV model tests, and thank CeSOS and NTNU for financial support.

References

[1] Vandiver, J. K., and Li, L., 2007. Shear7 v4.5 Program Theoretical Manual. Massachusetts Institute of Technology, Cambridge, USA.

[2] Triantafyllou, M., Triantafyllou, G., Tein, Y. D., and Ambrose, B. D., 1999. "Pragmatic riser viv analysis". In Offshore Technology Conference, no. OTC-10931-MS.

[3] MARINTEK, 2017. VIVANA Theory Manual v4.8.9. Trondheim, Norway, March.

[4] Gopalkrishnan, R., 1993. "Vortex-induced forces on oscillating bluff cylinders". PhD thesis, Massachusetts Institute of Technology, Cambridge, MA, USA.

[5] Aronsen, K. H., 2007. "An Experimental Investigation of In-line and Combined In-line and Cross-flow Vortex Induced Vibrations". PhD thesis, Norwegian University of Science and Technology, Trondheim, Norway.

[6] Dahl, J. M., Hover, F. S., and Triantafyllou, M. S., 2006. "Two degree-of-freedom vortex induced vibartions using a force assisted apparatus". Journal of Fluids and Structures, 22, pp. 807–818.

[7] Yin, D., 2013. "Experimental and numerical analysis of combined in-line and cross-flow vortex-induced vibrations". PhD thesis, Norwegian University of Science and Technology, Trondheim, Norway.

[8] Soni, P. K., 2008. "Hydrodynamic coefficients for vortex-induced vibrations of flexible beams". PhD thesis, Norwegian University of Science and Technology, Trondheim, Norway.

[9] Aglen, I. M., 2013. "VIV in free spanning pipelines". PhD thesis, Norwegian University of Science and Technology, Trondheim, Norway.

[10] Yin, D., and Larsen, C. M., 2010. "On determination of VIV coefficients under shear flow condition". In ASME 2010 29th International Conference on Ocean, Offshore and Arctic Engineering, Vol. 6, pp. 547–556.

[11] Yin, D., and Larsen, C. M., 2011. "Experimental and numerical analysis of forced motion of a circular cylinder". In ASME 2011 30th International Conference on Ocean, Offshore and Arctic Engineering, Vol. 7, pp. 327–336.

[12] Yin, D., and Larsen, C. M., 2012. "Forced motion experiments with measured motions from flexible beam tests under uniform and sheared flows". In ASME 2012 31st International Conference on Ocean, Offshore and Arctic Engineering, Vol. 5, pp. 573–581.

[13] Trim, A., Braaten, H., Lie, H., and Tognarelli, M., 2005. "Experimental investigation of vortex-induced vibration of long marine risers". Journal of Fluids and Structures, 21(3), pp. 335 – 361.

[14] Vandiver, J. K., Jaiswal, V., and Jhingran, V., 2009. "Insights on vortex induced, traveling waves on long risers". Journal of Fluids and Structures, 25, pp. 641–653.
[15] Song, L., Fu, S., Zeng, Y., and Chen, Y., 2016. "Hydrodynamic forces and coefficients on flexible risers undergoing vortex-induced vibrations in uniform flow". Journal of Waterway, Port, Coastal, and Ocean Engineering, 142(4), p. 04016001.
[16] Wu, J., 2011. "Hydrodynamic force identification from stochastic vortex induced vibration experiments with slender beams". PhD thesis, Norwegian University of Science and Technology, Trondheim, Norway.
[17] Bourguet, R., Karniadakis, G. E., and Triantafyllou, M. S., 2013. "Multi-frequency vortex-induced vibrations of a long tensioned beam in linear and exponential shear flows". Journal of Fluids and Structures, 41, pp. 33 – 42.
[18] NTNU. Marine cybernetics laboratory (MC-lab). See also URL www.ntnu.edu/imt/lab/cybernetics.
[19] Chaplin, J., Bearman, P., Huarte, F. H., and Pattenden, R., 2005. "Laboratory measurements of vortex-induced vibrations of a vertical tension riser in a stepped current". Journal of Fluids and Structures, 21(1), pp. 3 – 24.
[20] Passano, E., Larsen, C. M., and Lie, H., 2012. "Comparison of calculated in-line vortex induced vibrations to model tests". In ASME 2012 31st International Conference on Ocean, Offshore and Arctic Engineering, Vol. 5, pp. 705–712.